Journal of Medical Bacteriology

Evaluation of Cellular Toxicity, Residence Time, and Antibacterial Performance of Silver/Zinc Oxide Colloidal Nanostructures Coated on the Surface of Foley Catheters

Alireza Jafari [1, 2], Mohammad Naimi Joubani [3], Siavash Falahatkar [2], Sepide Roshani [2], Mahan Azizzade Dobakhshari [2]*

1 Current: Infectious Disease Research Center, Avicenna Institute of Clinical Sciences, Avicenna Health Research Institute, Hamadan University of Medical Sciences, Hamadan, Iran

2 Urology Research Center, Razi Hospital, School of Medicine, Guilan University of Medical Sciences, Rasht, Iran.

3 Research Center of Health and Environment, School of Health, Guilan University of Medical Sciences, Rasht, Iran.

ARTICLE INFO

Article type:
Research Article

Article history:

Received	01	Sep	2025
Revised	16	Sep	2025
Accepted	02	Oct	2025
Published	12	Dec	2025

Keywords:
Cellular toxicity, Antibacterial, Silver/Zinc oxide nanostructure, Catheter-associated urinary tract infections, Coating, Foley catheter, Escherichia coli.

*Corresponding Authors: Mahan Azizzade Dobakhshari: Urology Research Center, Razi Hospital, School of Medicine, Guilan University of Medical Sciences, Rasht, Iran. *Tel*: +98-13-33525259, *E-mail:* mahanazizzademaz@gmail.com.

ABSTRACT

Background: Catheter-associated urinary tract infections (CAUTIs) are a major cause of hospital-acquired infections, driven by biofilm-forming pathogens. Silver and zinc oxide nanoparticles offer synergistic antimicrobial effects. This study assesses a novel Ag-ZnO nanocomposite-coated catheter to improve efficacy, reduce cytotoxicity, and offer a cost-effective, locally-produced solution to combat CAUTIs.

Methods: Silver nanoparticles (AgNPs) and zinc oxide nanoparticles (ZnO-NPs) were synthesized via chemical reduction and sol-gel methods, respectively, and combined in a 2:8 ratio to form an antimicrobial nanocomposite. Foley catheters were functionalized through dip-coating and radiation-assisted drying. Nanostructures were characterized using DLS and TEM. Antibacterial activity was assessed through disk diffusion, microplate dilution (MIC/MBC), and log reduction assays against *E. coli*, *S. aureus*, and *P. aeruginosa*. Coated catheter efficacy was evaluated over 72 hours. Cytotoxicity was analyzed on L929 fibroblasts using the MTT assay.

Results: Silver-zinc oxide nanocomposites demonstrated moderate antibacterial activity, achieving a 0.65 log reduction in *Staphylococcus aureus* and 0.63 in *Pseudomonas aeruginosa*. Foley catheters coated with the nanocomposite showed complete inhibition of *E. coli* and *S. aureus* growth over 72 hours. Cytotoxicity assays revealed that ZnO nanostructures were non-toxic up to 1:16 dilution, while Ag nanoparticles exhibited dose-dependent cytotoxicity. The Ag-ZnO composite showed acceptable biocompatibility, maintaining over 70% L929 cell viability at 1:32 and 1:64 dilutions. These results support the potential of Ag-ZnO-coated catheters as antimicrobial devices with controlled cytotoxicity and broad-spectrum efficacy against common uropathogens.

Conclusion: The silver-zinc oxide nanocomposite demonstrated strong antibacterial activity against *P. aeruginosa*, *S. aureus*, and *E. coli*, with no cytotoxicity to L929 fibroblasts. These findings support its potential as a safe and effective antimicrobial coating for foley catheters, paving the way for future commercial production and clinical application.

- ***Please cite this paper as:*** Jafari A, Naimi Joubani M, Falahatkar S, Roshani S, Azizzade Dobakhshari M. Evaluation of Cellular Toxicity, Residence Time, and Antibacterial Performance of Silver/Zinc Oxide Colloidal Nanostructures Coated on the Surface of Foley Catheters. *J Med Bacteriol.* 2025; **13** (4): pp.13-24. DOI: 10.18502/jmb.v13i4.20520

Introduction

Urinary tract infections (UTIs) can affect any part of the urinary system, including the urethra, bladder, ureters, and kidneys. UTIs are the most common healthcare-associated infections reported to the National Healthcare Safety Network, with approximately 75% of hospital-acquired UTIs linked to urinary catheters (1). These catheters, which are tubes inserted through the urethra into the bladder to drain urine, are used in 15–25% of hospitalized patients during their stay. Prolonged catheterization is the primary risk factor for catheter-associated UTIs (CAUTIs), underscoring the need for strict adherence to indications and prompt removal when no longer necessary (1).

CAUTIs contribute to over 380,000 new infections annually and 9,000–13,000 deaths. Complications from these infections lead to prolonged hospitalizations, increased healthcare costs, and patient dissatisfaction. The pathogenesis of CAUTIs involves microbial adhesion to the catheter surface, colonization by pathogenic bacteria (e.g., Escherichia coli, *Staphylococcus aureus*, *Pseudomonas aeruginosa*), and subsequent biofilm formation. This biofilm facilitates bacterial migration to the bladder, exacerbating infection (2).

Current strategies to mitigate CAUTIs include catheter coatings impregnated with antibiotics, silver ions, hydrophobic materials, cationic agents, or antibacterial metal oxide nanostructures (3-5). Among these, silver nanoparticles (AgNPs) have re-emerged as a promising solution due to their broad-spectrum antimicrobial properties and historical use in wound care, water disinfection, and burn treatments (6). The antimicrobial mechanism of AgNPs involves: Binding to sulfur-containing membrane proteins, disrupting bacterial morphology and respiratory chains, Intracellular penetration, inactivation of vital enzymes, and hydrogen peroxide generation, Synergistic effects with zinc oxide nanoparticles (ZnO-NPs), enhancing activity against multidrug-resistant pathogens like Mycobacterium tuberculosis (7-11).

Similarly, zinc oxide nanoparticles (ZnO-NPs) exhibit potent antibacterial effects against Gram-positive and Gram-negative bacteria through: Reactive oxygen species (ROS) generation, even in dark conditions, release of Zn^{2+} ions, which interfere with bacterial metabolism and enzyme systems, direct membrane damage upon contact (12).

Combining AgNPs and ZnO-NPs has demonstrated synergistic antibacterial effects in animal models. For instance, a 512 µg/mL mixture significantly reduced *E. coli* colony counts in murine pyelonephritis models and mitigated kidney tissue damage (13). However, the cytotoxicity of nanostructures (<100 nm) to eukaryotic cells—particularly their ability to cross the blood-brain barrier (<35 nm)—remains a concern (14).

Despite advances, challenges persist in preventing biofilm formation on catheters. Recent innovations leverage nanotechnology to develop antimicrobial coatings that reduce bacterial adhesion and antibiotic resistance (15). This study evaluates a novel Foley catheter coated with Ag-ZnO nanocomposites, aiming to: Enhance antibacterial efficacy against CAUTI pathogens, Minimize eukaryotic cytotoxicity, Provide a cost-effective alternative to imported products (e.g., domestically produced AgNPs cost ~8× less than US-sourced equivalents).With rising hospital-acquired infections and antimicrobial resistance, such nanotechnology-driven solutions could revolutionize urological device markets, reduce healthcare burdens, and address unmet clinical needs.

Materials and Methods

Synthesis of Silver and Zinc Oxide Nanostructures

For the chemical reduction synthesis of colloidal silver nanoparticles (AgNPs), a 0.5 millimolar

silver nitrate ($AgNO_3$) solution was mixed with 0.02 molar sodium citrate, followed by addition of 0.01 molar sodium borohydride ($NaBH_4$, Merck, Germany) under constant magnetic stirring for 10 minutes. Zinc oxide nanoparticles (ZnO-NPs) were prepared by dissolving 0.2 molar zinc acetate dihydrate in methanol, then adding 1.2 molar sodium hydroxide in methanol under magnetic stirring for 3 hours, with subsequent centrifugation to remove macro-sized particles. Based on previous optimization studies (9), the final hybrid nanostructure was prepared by mixing 2 millilitre of colloidal AgNPs with 8 millilitre of colloidal ZnO-NPs to create an antibacterial nanocomposite.

Antimicrobial Ag–ZnO Coatings for Foley Catheters

The Foley catheter surface was functionalized through a multi-step coating process. Initially, colloidal solutions of silver nanoparticles (AgNPs) and zinc oxide nanoparticles (ZnO-NPs) were synthesized separately, then combined in a 2:8 volume ratio (Ag:ZnO). The catheter's external surface was first activated using diluted formaldehyde (3.7% v/v) for 5 minutes to generate reactive binding sites. The activated catheter was then dip-coated in the Ag-ZnO colloidal suspension for 10 minutes (immersion depth: 5 cm, withdrawal rate: 2 mm/s) to ensure uniform nanoparticle deposition. Immediately following coating, the catheter underwent radiation-assisted drying at 60 °C for 15 minutes (infrared lamp, 100 W intensity, 20 cm distance) to achieve stable nanoparticle adhesion while maintaining structural integrity of the polymer substrate. This process created a nanocomposite surface coating with demonstrated antimicrobial efficacy against common uropathogens while preserving catheter mechanical properties.

Characterization and Size Determination of Ag–ZnO Nanostructures

Dynamic Light Scattering (DLS) was used to calculate the polydispersity index (PDI) and determine the zeta potential of the nanostructures. Additionally, transmission electron microscopy (TEM) imaging was employed to estimate the approximate dimensions of the nanostructures. The size distribution and zeta potential were assessed using Dynamic Light Scattering (DLS). Since most nanostructures tend to agglomerate after synthesis, they must be dispersed before TEM observation. For sample preparation, the following procedure was adopted: A very small amount of the synthesized powder was placed in a vial containing an appropriate dispersant (e.g., ethanol, acetone, distilled water, etc.). It should be noted that the selected dispersant must not react chemically with the sample. The vial containing the nanostructures was then subjected to ultrasonication at an optimal power and duration (ranging from 1 to 30 minutes, depending on the sample) to deagglomerate the nanostructures. Subsequently, a few drops of the dispersed sample were pipetted onto a suitable TEM grid (the holder for nanostructures in transmission electron microscopy (TEM)). After 5 minutes, the dispersant evaporated from the grid, which was then transferred into the TEM for imaging.

Disk Diffusion Inhibition Zones for Ag, ZnO, and Ag–ZnO Nanostructures

The inhibition zone diameter was evaluated using the disk diffusion method by impregnating blank disks with colloidal nanostructures (16). For the disk diffusion assay, bacterial suspensions of *Escherichia coli* (*E. coli*) and *Staphylococcus aureus* (American Type Culture Collection [ATCC] 6538) were prepared to a 0.5 McFarland standard from 18-hour-old colonies. Using a sterile swab, the microbial suspension was inoculated onto the surface of Mueller-Hinton agar (MHA)

plates, and after 15 minutes, blank disks were placed on the agar. Following an additional 15 minutes, the plates were incubated at 35-37 °C (degrees Celsius) for 16-18 hours, after which the inhibition zone diameter was measured with a ruler.

Microplate Dilution Antibacterial Evaluation of Ag, ZnO, and Ag–ZnO Nanostructures

To evaluate the antibacterial effects of the synthesized nanostructures against *Escherichia coli* ATCC (American Type Culture Collection) 25922 and *Staphylococcus aureus* ATCC 6538 (lyophilized microbial strains from Bahar Afshan Company), the microtube dilution method (Microtube Dilution Method) was employed, wherein serial dilutions of each nanostructure were prepared and inoculated with a standardized bacterial suspension; the mixture of bacterial suspension and nanostructures in Mueller Hinton Broth (MHB) was exposed to ultrasonic (ultrasonic wave) treatment, and after incubation, bacterial susceptibility was assessed visually (via the naked eye), with the minimum inhibitory concentration (MIC, Minimum Inhibitory Concentration), the lowest nanostructure concentration inhibiting visible growth (indicating a bacteriostatic effect), being determined, followed by the minimum bactericidal concentration (MBC, Minimum Bactericidal Concentration), where 100 µL (microliter) aliquots from each well were plated onto solid culture medium, and a ≥99.9% reduction in colony count compared to the control plate confirmed the MBC.

Log Reduction Assessment of P. aeruginosa and S. aureus with Ag–ZnO Nanostructures

To evaluate the log reduction of *Pseudomonas aeruginosa* ATCC (American Type Culture Collection) 27853 and *Staphylococcus aureus* ATCC 6538 (obtained from Bahar Afshan Company) following exposure to silver-zinc oxide nanostructures, 100 microliters (µL) of bacterial suspension (1×10^3 colony-forming units [CFU]/mL) was added to microplate wells containing 1 milliliter (mL) of serially diluted nanostructures, with samples collected at 0, 5, and 10 minutes using sterile swabs and plated on Trypticase Soy Agar (TSA) for enumeration; bacterial counts (CFU/plate) were compared against both negative (sterile TSA) and positive (bacteria-inoculated TSA) controls to determine antimicrobial efficacy, with log reduction calculated as $\log_{1\ 0}(N_0/N)$ where N_0 represents control CFU and N represents post-treatment CFU.

Antibacterial Evaluation of Ag–ZnO–Coated Foley Catheter Surfaces

To evaluate the antibacterial activity of the external surface of a labeled Foley catheter coated with silver (Ag) and zinc oxide (ZnO) nanostructures, the catheter's external surface was first activated using diluted formaldehyde and then functionalized via dip coating by immersing it in colloidal Ag-ZnO nanostructures for 10 minutes, followed by immediate drying under 60 °C radiative heating for 15 minutes; the coated catheter was then exposed to bacterial suspensions (1×10^3 CFU/mL) of *Pseudomonas aeruginosa* ATCC (American Type Culture Collection) 27853 and *Staphylococcus aureus* ATCC 6538 in an isolated environment, with sterile swab samples collected from the catheter surface at 0, 24, 48, and 72 hours for microbial enumeration on Trypticase Soy Agar (TSA) plates, where colony-forming unit (CFU/plate) counts were recorded and analyzed to determine antibacterial efficacy.

Cytotoxicity Evaluation of Silver-Zinc Oxide Nanostructures Against L929 Cells Using MTT Assay

The cytotoxicity of silver (Ag) and zinc oxide (ZnO) nanostructures (active substance) against L929 fibroblast cells was evaluated using the MTT

(3-(4,5-dimethylthiazol-2-yl)-2,5-diphenyltetrazolium bromide) assay by Kia Nano Bio Vista Company in accordance with ISO (International Organization for Standardization) 10993-5:2009, where extraction was performed following ISO 10993-12 guidelines; for sample preparation, 1 milliliter (mL) of culture medium was added per 0.2 mL of test sample and incubated at 37±1°C for 24±2 hours, with extracts prepared from varying dilutions of Ag nanostructures, ZnO nanostructures, and a 2:8 volumetric mixture of Ag-ZnO nanostructures. Subsequently, L929 cells (1×10^4 cells/well) were seeded in 96-well plates with RPMI (Roswell Park Memorial Institute) medium (supplemented with 10% fetal bovine serum [FBS], 1% penicillin-streptomycin) in six replicates and incubated for 24±2 hours at 37±1 °C with 5% carbon dioxide (CO_2) to allow cell adhesion, after which the medium was replaced with nanostructure extracts and cells were exposed for an additional 24±2 hours. Following incubation, 50 microliters (µL) of MTT dye (Sigma-Aldrich, 1 milligram per milliliter [mg/mL]) was added to each well, and after 2 hours, the dye was removed and replaced with isopropanol to dissolve the formed purple formazan crystals via 5-minute shaking, with optical density (OD) measured at 570 nanometers (nm) using an ELISA reader (BioTek, USA). Viable cells exhibited higher OD values than nonviable cells, and cell viability percentage was calculated as [(OD of test)/(OD of control)]×100, with data plotted using Microsoft Excel; control groups consisted of L929 cells cultured without nanostructures.

Results

Identification and Size Estimation of Nanostructures

The dynamic light scattering (DLS) measurements were performed using a stereoscope (Stereoscope-IN A-ONE Enc., Korea). The intensity distribution spectra revealed that the hydrodynamic diameter ranges of the colloidal silver and zinc oxide nanostructures were approximately 24.4 nm and 52.48 nm, respectively. The polydispersity index (PDI, a measure of particle size distribution uniformity) was calculated for the silver and zinc oxide nanostructures, with estimated values of 1 and 0.667, respectively. A PDI closer to 1 indicates monodispersity (uniform particle size), while values farther from 1 suggest polydispersity (heterogeneous size distribution). The results demonstrated that both silver and zinc oxide nanostructures exhibited homogeneous populations. Additionally, the instrument measured the zeta potential (ζ-potential, an indicator of colloidal stability) of the silver and zinc oxide nanostructures as −20.7 mV and −0.709 mV, respectively. The more negative zeta potential of the silver nanostructures enhances mutual electrostatic repulsion, thereby promoting long-term stability and preventing agglomeration of both silver and zinc oxide nanostructures. (Table 1).

The measurement of elements was conducted using the Inductively Coupled Plasma Optical Emission Spectrometry (ICP-OES) 730-ES, Varian device at the accredited laboratory services center of Sharif University of Technology, which is approved by the Food and Drug Administration of Iran. ICP-OES, known for its ability to perform simultaneous multi-element analysis, is the most suitable method for detecting mineral nanostructures. In this experiment, the concentration of silver nanostructures and zinc oxide nanostructures was analyzed.

According to the recorded results, the concentration of colloidal silver nanostructures in an aqueous solvent was approximately 25 parts per million (ppm), while the concentration of zinc oxide nanostructures was measured at around 70 ppm.

Table 1 Identification analysis and size estimation of zinc oxide nanostructures.

Comments	Values	Identification Analysis and Size Estimation of Zinc Oxide Nanostructures
The closer the PDI (Polydispersity Index) values are to 1, the more monodisperse the synthesized nanoparticles are. Conversely, the further the obtained PDI values deviate from 1, the more polydisperse the nanoparticles become.	0.667	Poly dispersity index (PDI)
A more negative zeta potential helps zinc oxide nanostructures repel each other more strongly, thereby enhancing long-term stability and preventing agglomeration of the ZnO nanostructures.	-0.709 mv	Zeta potensial
	52.48 nm	Dynamic Diameter Range
	20-30 nm	Measurement of elements by ICP-OES-
In the TEM images, the zinc oxide nanostructures appear as spherical balls with smooth surfaces and a clustered spatial arrangement. The transmission electron microscopy (TEM) images show that abnormal states in the shape and size of the synthesized nanostructures are rarely observed.	Approximately 0.88 ± 14.16	Analysis of Transmission Electron Microscope (TEM) Images

Table 2. Antibacterial effects of silver nanostructures, zinc oxide nanostructures, and their hybrid mixture against standard strains of *E. coli* and *S. aureus* using disk diffusion and microplate dilution methods.

		DIZ (mm)	MIC (µg/ml)	MBC (µg/ml)
Ag NPs	*E. coli*	2	0.19 (Cavity: 6^{th}, 1/64)	0.39 (Cavity: 5^{th}, 1/32)
	Staphylococcus aureus	0	0.39 (Cavity: 5^{th}, 1/32)	0.78 (Cavity: 4^{th}, 1/16)
ZnO NPs	*E. coli*	10	0.203 (Cavity: 8^{th} 1/256)	1.62 (Cavity: 5^{th} 1/32)
	Staphylococcus aureus	10	0.406 (Cavity: 7^{th}, 1/128)	1.62 (Cavity: 5^{th} 1/32)
AgZnO NPs	*E. coli*	18	0.149 (Cavity: 9^{th}, 1/512)	0.601 (Cavity: 7^{th}, 1/128)
	Staphylococcus aureus	15	0.149 (Cavity: 9^{th}, 1/512)	0.601 (Cavity: 7^{th}, 1/128)

Table 3. Evaluation of log reduction of the standard strains *Pseudomonas aeruginosa* and *Staphylococcus aureus* in the presence of the active ingredient mixture of silver and zinc oxide nanostructures.

Average test results AgZnO	Averege forming colony on TSA (CFU/Plate)			
	Time 0	After 5 min	After 10 min	Log Reduction After 10 min
Pseudomonas aeruginosa	1.0×10^3	260	235	0.63 Log
Staphylococcus aureus	1.0×10^3	235	220	0.65 Log

Table 4. Evaluation of the antibacterial effect of the outer surface of a labeled Foley catheter coated with silver and zinc oxide nanostructures against standard bacterial strains.

Average test results AgZnO		Growth of forming colony on TSA (CFU/Plate)			
	Start inoculum	Time 0	24 hours	48 hours	72 hours
E. coli	1.0×10^3	1.0×10^3	No growth	No growth	No growth
Staphylococcus aureus	1.0×10^3	1.0×10^3	No growth	No growth	No growth

Table 5. Percentage of viable cells (SF,Surviving Fraction) and inhibited cells (GI, Growth Inhibition) of L929 fibroblasts after 24-hour exposure to silver (Ag), zinc oxide (ZnO), and mixed silver/zinc oxide (Ag/ZnO) nanostructures, compared to the control group.

Concentr-ation of nano-structures of	1:2	1:4	1:8	1:16	1:32	1:64	control
ZnO %SF %GI	0.242±0.006** 30.94 % 69.05 %	0.356±0.011** 45.52 % 54.47	0.419±0.027** 53.58% 46.41%	0.610±0.010** 78.00% 21.99%	0.715±0.013*** 91.43% 8.56%	0.779±0.009*** 99.61% 0.38%	0.782±0.006 100% 0%
Ag SF% %GI	0.103±0.006** 18.65% 81.34%	0.150±0.009** 27.17% 72.82%	0.203±0.015** 36.77% 63.22%	0.246±0.011** 44.56% 55.43%	0.302±0.007** 54.71% 45.28%	0.345±0.005** 62.5% 37.5%	0.552±0.010 100% 0%
Ag/ZnO %SF %GI	0.226±0.025** 28.78% 71.21%	0.236±0.032** 30.06% 69.93%	0.303±0.251** 38.59% 61.41%	0.360±0.055** 45.85% 54.14%	0.786±0.040*** 100.12% 0%	0.830±0.052*** 105.73% 0%	0.785±0.213 100% 0%

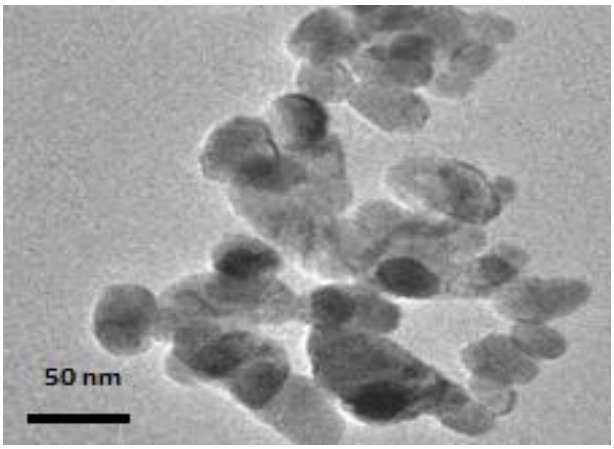

Figure 1. TEM image of silver nano-structures at 460 K magnification (scale bar: 50 nm).

The morphology of the synthesized silver nanostructures and zinc oxide nanostructures obtained from transmission electron microscopy (TEM) is displayed in Figure 1 and Figure 2, respectively. The silver nanostructures exhibit a spherical volume with a smooth surface morphology, while the zinc oxide nanostructures appear aggregated, forming a clumped structure. The TEM images reveal that irregular shapes and sizes are rarely observed in the synthesized nanostructures. The average size of the silver nanostructures, as determined by the DLS (Dynamic Light Scattering) analyzer software, was estimated to be approximately 13 ± 3.14 nm (Figure 1), whereas the zinc oxide nanostructures measured around 14.16 ± 0.88 nm (Figure 2).

Evaluation of Antibacterial Effects

The results of antimicrobial tests on silver nanostructures revealed that they exhibited very weak antibacterial properties against the standard strain of Escherichia coli (stands for Escherichia coli), with the minimum inhibitory concentration (MIC, stands for Minimum Inhibitory Concentration) measured at approximately 0.19 µg/mL (Cavity: 5th, 1/64), while the minimum bactericidal concentration (MBC, stands for Minimum Bactericidal Concentration) was calculated at around 0.39 µg/mL (Cavity: 6th, 1/32), indicating their low efficacy at various dilutions against E. coli.

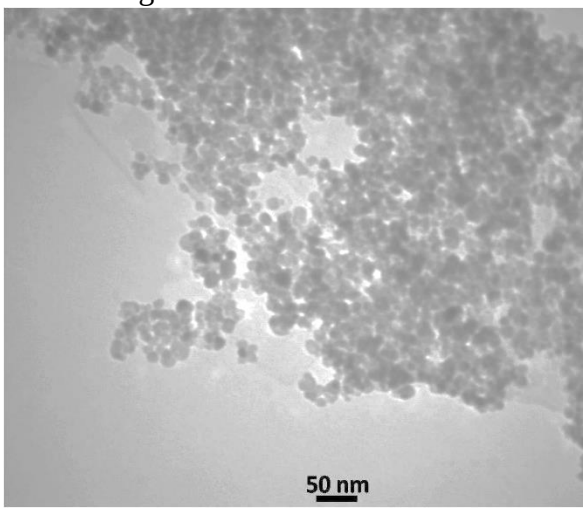

Figure 2. TEM image of zinc oxide (ZnO) nanostructures at 200K magnification (scale bar: 50 nm).

Similarly, silver nanostructures showed very weak antibacterial activity against the standard strain of *Staphylococcus aureus* (stands for *Staphylococcus aureus*), with an MIC of approximately 0.39 µg/mL (Cavity: 6th, 1/32) and an MBC of about 0.78 µg/mL (Cavity: 5th, 1/16), further confirming their limited effectiveness. In contrast, zinc oxide (ZnO) nanostructures demonstrated relatively strong antibacterial properties against *E. coli*, with an MIC of 0.203 µg/mL (Cavity: 8th, 1/256) and an MBC of 1.62 µg/mL (Cavity: 5th, 1/32), suggesting acceptable efficacy. Against *S. aureus*, ZnO nanostructures also exhibited relatively potent antibacterial activity, with an MIC of 0.406 µg/mL (Cavity: 7th, 1/128) and an MBC of 1.62 µg/mL (Cavity: 5th, 1/32). Notably, the mixture of silver and zinc oxide nanostructures displayed highly potent antibacterial effects against *E. coli*, with an MIC of 0.149 µg/mL (Cavity: 9th, 1/512) and an MBC of 0.601 µg/mL (Cavity: 7th, 1/128), as well as against S. aureus, with identical MIC and MBC values (0.149 µg/mL and 0.601 µg/mL,

respectively), underscoring their strong antimicrobial performance at various dilutions (Table 2).

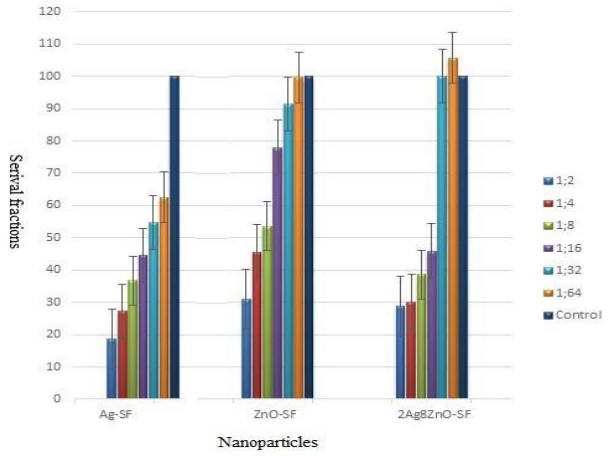

Figure 3. Percentage of viable L929 cells following 24-hour exposure to silver (Ag), zinc oxide (ZnO), and silver/zinc oxide (Ag/ZnO) mixed nanostructures compared to control group.

The test to determine the log reduction of the standard strains *Pseudomonas aeruginosa* and *Staphylococcus aureus* in the presence of the active ingredient, a mixture of silver and zinc oxide nanostructures, was conducted at Niko Pharmad. Based on the obtained results, the mixture of silver and zinc oxide nanostructures, when exposed to *Staphylococcus aureus*, achieved a 0.65 logarithmic reduction in the number of colonies formed on the plate containing Tryptic Soy Agar (TSA) culture medium. Similarly, the mixture of silver and zinc oxide nanostructures, when exposed to *Pseudomonas aeruginosa*, achieved a 0.63 logarithmic reduction in the number of colonies formed on the plate containing Tryptic Soy Agar (TSA) culture medium (Table 3).

Antibacterial Evaluation of Foley Catheters Coated with Ag–ZnO Nanostructures

Based on the obtained evidence, the results of microbial cultures prepared from the external surface of a Foley catheter coated with a mixture of silver and zinc oxide nanostructures in the presence of *Staphylococcus aureus* (*S. aureus*) and *Escherichia coli* (*E. coli*) indicated negative bacterial growth on the surface of the tryptic soy agar (TSA) plate after 24 hours, 48 hours, and 72 hours of incubation. (Table 4).

MTT (3-(4,5-dimethylthiazol-2-yl)-2,5-diphenyltetrazolium bromide) Cytotoxicity Evaluation of Ag, ZnO, and Ag–ZnO Nanostructures on L929 Cells

The cytotoxicity assays of silver and zinc oxide nanostructures against L929 fibroblast cell line were conducted (Figures 1, Table 5). According to the results, more than 70% of the cells remained viable at a 1:16 dilution of the initial suspension when exposed to zinc oxide (ZnO) nanostructures compared to the control group. The findings indicated that when the concentration of nanostructures was reduced to a 1:32 dilution of the initial suspension, the viability of cells in the culture medium increased further, with approximately 100% of L929 fibroblast cells still viable at this dilution. This evidence suggested that zinc oxide nanostructures exhibited no toxic effects against L929 cells at concentrations up to a 1:16 dilution of the initial suspension (Figures 1, Table 5). In contrast, silver (Ag) nanostructures demonstrated significantly different behavior, exhibiting cytotoxicity against L929 fibroblast cells at all tested dilutions (Figures 1, Table 5). When exposed to a mixture of silver and zinc oxide nanostructures, more than 70% of the cells remained viable at dilutions of 1:32 and 1:64, indicating no cytotoxic activity against the cells at these concentrations (Figures 1, Table 5).

Discussion

In this study, silver (Ag) and zinc oxide (ZnO) nanostructures were synthesized and subsequently mixed at a 2:8 volume ratio. The constituent elements were characterized using dynamic light scattering (DLS), inductively coupled plasma optical emission spectroscopy (ICP-OES), and transmission electron microscopy (TEM) to determine size distribution, zeta potential, dimensional estimates, and concentration quantification. The Foley catheter surface was then functionalized with the Ag-ZnO nanocomposite using dip-coating methodology. Antimicrobial efficacy was evaluated against standard bacterial strains through disk diffusion assays and microplate dilution methods, with particular focus on quantifying the logarithmic reduction in colony-forming units (CFUs) of *Pseudomonas aeruginosa* and *Staphylococcus aureus*. Cytocompatibility was assessed via methylthiazolyldiphenyl-tetrazolium bromide (MTT) assay using L929 fibroblast cells.

Size distribution analysis revealed hydrodynamic diameters of 24.4 nm for colloidal silver nanostructures and 52.48 nm for zinc oxide nanostructures, with polydispersity indices (PDI) of 1 and 0.667 respectively, indicating monodisperse populations. Zeta potential measurements recorded -20.7 mV for Ag and -0.709 mV for ZnO nanostructures. ICP-OES quantification determined concentrations of 25 parts per million (ppm) for silver and 70 ppm for zinc oxide nanostructures in aqueous suspension. TEM imaging confirmed spherical Ag nanoparticles with smooth morphology, while ZnO nanostructures exhibited clustered aggregates. Digital analysis software (DJMizer) calculated mean particle sizes of 13 ± 3.14 nm (Ag) and 14.16 ± 0.88 nm (ZnO).

Our findings contrast with several previous reports. Lethongkam et al. demonstrated that eucalyptus (*E. camaldulensis*)-mediated Ag nanoparticle-coated urinary catheters (20-120 nm by scanning electron microscopy/SEM) significantly prevented microbial adhesion and biofilm formation in human urine models (17). Similarly, Roe et al. documented pronounced antimicrobial activity of radiolabeled Ag nanoparticles (3-18 nm, mean 10.7 nm) on Foley catheters, achieving 67% inhibition of *P. aeruginosa* and near-complete suppression of *S. aureus* and *Escherichia coli* over 72 hours (18). Goda RM 's team reported 15-25 nm spherical Ag nanoparticles (synthesized using *Pistacia lentiscus*) that effectively inhibited both Gram-positive and Gram-negative pathogens (19). The observed dimensional variations (our study: 13-14.16 nm) likely stem from divergent synthesis protocols, laboratory conditions, reagent purity, and optimization expertise.

Notably, our antimicrobial assays (disk diffusion, minimum inhibitory concentration/MIC, minimum bactericidal concentration/MBC) revealed weaker antibacterial properties of Ag nanostructures against *E. coli* and *S. aureus* compared to ZnO. However, the 2:8 Ag-ZnO nanocomposite exhibited synergistic effects, achieving logarithmic reductions of 0.65 CFU for *S. aureus* and 0.63 CFU for *P. aeruginosa* on tryptic soy agar (TSA) plates. This enhancement correlates with the higher ionic concentration (70 vs 25 ppm) and greater Zn^{2+} release measured by ICP-OES, supporting the concentration-dependent antimicrobial mechanism proposed by Wu et al., who correlated bactericidal efficacy with aqueous metal ion availability (20).

The divergent outcomes compared to literature may reflect: Differential nanoparticle release kinetics from catheter surfaces, strain-specific susceptibility variations, methodological differences in biofilm modeling, distinct physiochemical properties arising from our composite approach.

While Goda et al. reported superior Ag nanoparticle efficacy against Gram-negatives (19), our nanocomposite demonstrated balanced

activity against both Gram classes, suggesting ZnO's role in broadening the antimicrobial spectrum. The sustained 72-hour inhibition observed across studies, including ours, underscores the potential for extended clinical protection.

Conclusion

The active component, a mixture of silver nanostructures and zinc oxide (ZnO) nanoparticles, exhibits significant antibacterial activity against *Pseudomonas aeruginosa*, *Staphylococcus aureus*, and *Escherichia coli* (*E. coli*), while demonstrating no cytotoxic effects on L929 fibroblast cells. It is hoped that in the near future, we will witness the commercial production of silver-zinc oxide nanostructure-coated Foley catheters with potent antibacterial properties.

Acknowledgements

We would like to thank Guilan University of Medical Sciences for his assistance and guidance in this research.

Funding Information

The author(s) received no specific funding for this work.

Ethics approval and consent to participate

This study was conducted in accordance with the ethical principles outlined in the Declaration of Helsinki. Prior to conducting the study, all necessary approvals were obtained from the Ethics Committee of Guilan University of Medical Sciences. The research protocol and procedures involving human participants were reviewed and approved by the Ethics Committee of Guilan University of Medical Sciences (IR.GUMS.REC.1400.207). Adhering to these ethical guidelines ensures the protection of the rights, welfare, and well-being of the study participants.

Conflict of interest

The authors declare that they have no competing interests.

References

1. Tambyah PA, Oon J. Catheter-associated urinary tract infection. *Curr Opin Infect Dis* 2012; **25**(4):365-70.
2. Shuman EK, Chenoweth CE. Urinary catheter-associated infections. *Infect Dis Clin* 2018; **32**(4):885-97.
3. Dayyoub E, Frant M, Pinnapireddy SR, et al. Antibacterial and anti-encrustation biodegradable polymer coating for urinary catheter. *Int J Pharm* 2017; **531**(1):205-14.
4. Mandakhalikar KD, Wang R, Rahmat JN, et al. Restriction of in vivo infection by antifouling coating on urinary catheter with controllable and sustained silver release: a proof of concept study. *BMC Infect Dis* 2018; **18**(1):370.
5. Bhargava A, Pareek V, Roy Choudhury S, et al. Superior bactericidal efficacy of fucose-functionalized silver nanoparticles against *Pseudomonas aeruginosa* PAO1 and prevention of its colonization on urinary catheters. *ACS Appl Mater Interfaces* 2018; **10**(35):29325-37.
6. Moyer CA, Brentano L, Gravens Dl, et al. Treatment of large human burns with 0.5% silver nitrate solution. *Arch Surgery* 1965; **90**(6):812-67.
7. Mirershadi F, Jafari A, Janati E, et al. Ag/ZnO Nano-composites as novel antibacterial agent against strain of MRSA. *Pure Appl Microbio* 2013; **7**:947–56.
8. Jafari A, Ghane M, Arastoo SH. Synergistic antibacterial effects of nano zinc oxide combined with silver nanocrystales. *Afr J Microbiol Res* 2011; **5**(30):5465-73.
9. Jafari A, Mosavari N, Movahedzadeh F, et al.

Bactericidal impact of Ag, ZnO and mixed AgZnO colloidal nanoparticles on H37Rv *Mycobacterium tuberculosis* phagocytized by THP-1 cell lines. *Microb Pathog* 2017; **110**:335-44.
10. Jafari A, Jafari Nodooshan S, Safarkar R, et al. Toxicity effects of AgZnO nanoparticles and rifampicin on *Mycobacterium tuberculosis* into the macrophage. *J Basic Microbiol* 2018; **58**(1):41-51.
11. Heidary M, Zaker Bostanabad S, Amini SM, et al. The anti-mycobacterial activity of Ag, ZnO, and Ag-ZnO nanoparticles against MDR-and XDR-*Mycobacterium tuberculosis*. *Infect Drug Resist* 2019; **12**:3425-35.
12. Siddiqi KS, Ur Rahman A, Tajuddin N, et al. Properties of zinc oxide nanoparticles and their activity against microbes. *Nanoscale Res Lett* 2018; **13**(1):141.
13. Khoshkbejari MAP, Jafari A, Safari M. Ag/ZnO nanoparticles as novel antibacterial agent against of *Escherichia coli* infection, in vitro & in vivo. *Orient J Chem* 2015; **31**(3):1437.
14. Dawson KA, Salvati A, Lynch I. Nanoparticles reconstruct lipids. *Nat Nanotechnol* 2009; **4**(2):84-5.
15. Borrego B, Lorenzo G, Mota-Morales JD, et al. Potential application of silver nanoparticles to control the infectivity of Rift Valley fever virus in vitro and in vivo. *Nanomedicine* 2016; **12**(5):1185–92.
16. Wayne P. Performance standards for antimicrobial susceptibility testing, ninth informational supplement. 2008;
17. Lethongkam S, Paosen S, Bilhman S, et al. *Eucalyptus*-mediated synthesized silver nanoparticles-coated urinary catheter inhibits microbial migration and biofilm formation. *Nanomaterials* 2022; **12**(22):4059.
18. Roe D, Karandikar B, Bonn-Savage N, et al. Antimicrobial surface functionalization of plastic catheters by silver nanoparticles. *J Antimicrob Chemother* 2008; **61**(4):869-76.
19. Goda RM, El-Baz AM, Khalaf EM, et al. Combating bacterial biofilm formation in urinary catheter by green silver nanoparticle. *Antibiotics* 2022; **11**(4):495.
20. Wu K, Yang Y, Zhang Y, et al. Antimicrobial activity and cytocompatibility of silver nanoparticles coated catheters via a biomimetic surface functionalization strategy. *Int J Nanomedicine* 2015; **10**:7241-52.